

## Supporting Information

**SI 1. Endotoxin removal from gelatin.** 100 mg of type B gelatin powder was dissolved in 10 ml of sterile deionized water and 100 $\mu$ l Triton<sup>TM</sup> X-114 (1%) was added into the gelatin solution by vigorous vortexing. Samples were placed in ice bath for 15 min to ensure a homogenous solution. After vortexing chilled samples, the tubes were warmed to 37 °C in water bath for 30 min to allow two phases to form. Samples were then centrifuged at 3,000 rpm for 1 min. After centrifugation, detergent phase stayed at the bottom of tube as an oily droplet. Upper aqueous phase was removed with care. This process was repeated three times to remove endotoxin completely. The gelatin solution was freeze-dried and stored at 4°C. Dried gelatin was dissolved in sterile water at 1 mg/ml. Endotoxin level of gelatin solution was tested with ToxinSensor<sup>TM</sup> Chromogenic L-amebocyte lysate (LAL) Endotoxin Assay Kit (GenScript, NJ, USA). The endotoxin free gelatin was used for all further nanoparticle formulation.

**SI 2. Synthesis of thiolated gelatin.** Briefly, 1 g of type B gelatin was dissolved in 100 mL deionized water and was allowed to react overnight with 20 mg of 2-iminothiolane hydrochloride at room temperature. The unreacted reagents were removed from the product by dialyzing against 5 mM HCl followed by 1 mM HCl solution for 3 hours each and finally against deionized water overnight. The purified thiolated gelatin was freeze dried and stored at 4 °C until further use. Ellman's reagent (5,5'-dithiobis-(2-nitrobenzoic acid)) was used to estimate free sulfhydryl groups as a measure of degree of thiolation, in which reagent reacts with free sulfhydryl groups to produce a mixed disulfide and 2-nitro-5-thiobenzoic acid, yellow colored compound with the absorbance at 412 nm.

**SI 3. Synthesis of non-targeted and EGFR-targeted gelatin nanoparticles.** 200 mg thiolated gelatin was dissolved in water and pH of solution was adjusted to 7 by addition of 0.2 M NaOH solution. 1mg DNA was added and gently mixed with gelatin solution. Chilled ethanol (incubated at -20 °C for 1 h) was added slowly into the mixture while stirring solution at 600 rpm using magnetic bead. Nanoparticles were formed when solvent composition changed to 75% hydro-alcoholic solution. The nanoparticles were further cross-linked by slow addition of 0.1 ml 8% (v/v) glyoxal solution. Unreacted reagents were quenched with 0.5 ml 0.2 M glycine solution. The gelatin nanoparticles were ultra-centrifuged at 16,000 rpm for 30 m. Pellets were washed with deionized water twice and purified nanoparticles were freeze-dried and stored at 4 °C until used. A similar process was used for synthesis of gemcitabine encapsulated gelatin nanoparticles, where drug-conjugated gelatin was dissolved in deionized water (1% w/v) at 37 °C.

The purified nanoparticles were suspended in 0.1 M phosphate buffer (pH 7.4) at a concentration of 10 mg/ml and modified with mPEG-SCM (MW 2,000 Da) or MAL-PEG-SCM (MW 2,000 Da) for 2 hours at room temperature with slow stirring. MAL-PEG-SCM-modified nanoparticles were re-suspended in 0.1 M phosphate buffer (pH 6.5) at a concentration of 10 mg/ml and incubated with 10% weight of 12 amino acid EGFR binding peptide flanked with four glycine spacer and a terminal cysteine (i.e., **Y-H-W-Y-G-Y-T-P-Q-N-V-I-G-G-G-G-C**) for 6 hours at room temperature. The reaction between the terminal maleimide residue of PEG with the

thiol residue of the cysteine in the peptide allows for tethering of the peptide from the nanoparticle surface for flexible interactions with EGFR. The peptide-modified nanoparticles were collected by ultra-centrifugation at 16,000 rpm for 30 minutes, washed, freeze-dried and stored at 4 °C until used.

#### SI 4. Size distribution of the Gem-Gel nanoparticles.

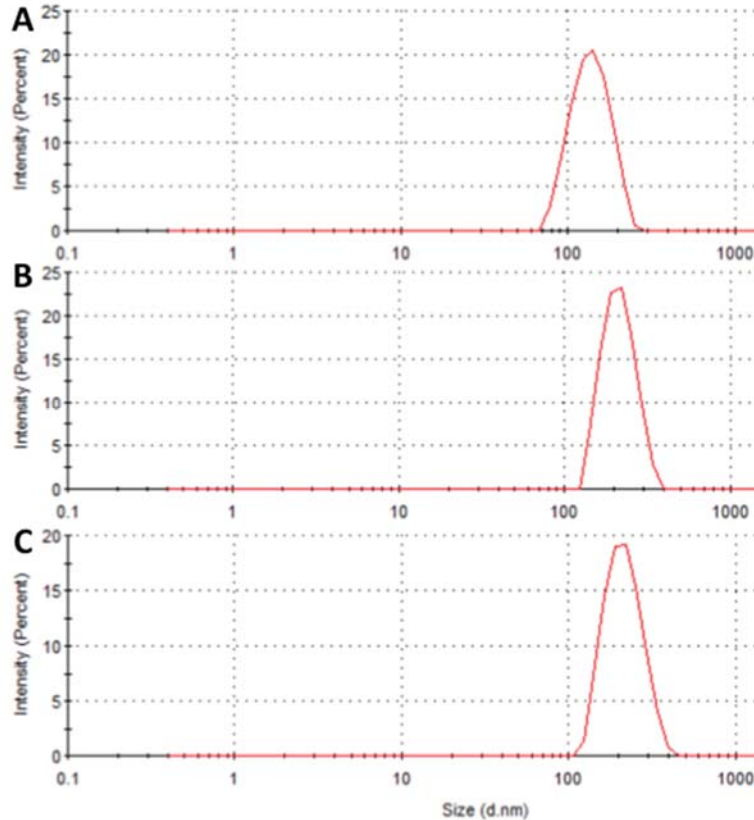


**Figure SI 4.** Representative size distribution plots of gemcitabine encapsulated (A) Gel, (B) Gel-PEG and Gel-PEG-EGFR nanoparticles showing unimodal distribution. All size measurements were performed three times and corresponding size with standard deviation has been reported in Table 1 of the manuscript.

**SI 5. Evaluation of EGFR expression in Panc-1 and Panc-1 luc cells.** Prior to their use, the Panc-1 luc cells were assessed for their EGFR-expression by western blot analysis, which revealed that the cells carry a high expression of the receptor, similar to native Panc-1 cells. Concentration of total protein collected from cell lysates of 2 million cells was analyzed by BCA assay (Pierce, Rockford, IL). Twenty-five micrograms of total protein extract was run on 7.5 % pre-cast SDS-PAGE for 20 m at 200 V. The protein bands from gel were transferred onto PVDF membrane by iBlot® Dry Blotting System (Invitrogen, Carlsbad, CA). Membrane was blocked with 5% BSA in Tween®-containing Tris buffer saline (TBS-t) for 1 hour at room temperature followed by incubation in 1:500 dilution of primary mouse  $\beta$ -actin antibody and 1:1000 dilution of primary rabbit EGFR antibody separately overnight at 4 C. Membrane was washed three

times with TBS-t and incubated with 1:2000 dilution of secondary anti-rabbit or anti-mouse horse-radish peroxidase-conjugated IgG in TBS-t for 1 hour at room temperature. After washing with TBS-t (3 times) and water, the membrane was exposed to 4 ml ECL substrate (Pierce, Rockford, IL) for 5 minutes. The chemiluminescent bands were visualized using *In Vivo* FX imaging station (Rochester, NY) for 5 min.  $\beta$ -actin was used as the protein loading control.

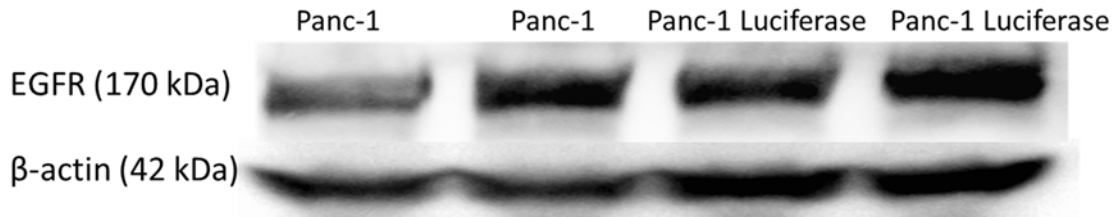


**Figure SI 5.** Western blot analysis of Panc-1 and Panc-1 luc cells to confirm the EGFR expression.  $\beta$ -actin was used as the protein loading control.

**SI 6. Evaluation of luciferase activity of Panc-1 luc cells.** The surgical orthotopic Panc-1 pancreatic adenocarcinoma model was developed in both nude (*nu/nu*) and severe combined immunodeficiency (SCID) mice to study the timeline of tumor growth and induction of metastasis. Luciferase-expressing Panc-1 cells (Panc-1 luc) were used instead of regular Panc-1 cells in order to study the tumor implantation and growth as a function of enzymatic activity, which could be evaluated by live imaging of the animals. *In vitro* bioluminescence activity of the Panc-1 luc cells was evaluated as a function of number of cells to ascertain that the signal response increases linearly with the increase in the total number of cells. We were able to obtain a detectable signal from 1250 Panc-1 luc cells by using Kodak In Vivo FX imaging station, while the Lumina II IVIS imaging system demonstrated better sensitivity and was able to pick signal from as low as 600 cells (Supporting information, SI 3). The calibration curves (Supporting information, Figure SI 2B & D) obtained from the IVIS and Kodak imaging system showed a positive correlation between the luminescence intensity signal and the number of cells, which was in agreement with the previous report where the luciferase expression from the cells was reported to be highly stable even after 3 months of sub-culturing. Lumina II IVIS was selected as the imaging modality of choice for the *in vivo* studies, since it provides a better signal sensitivity.

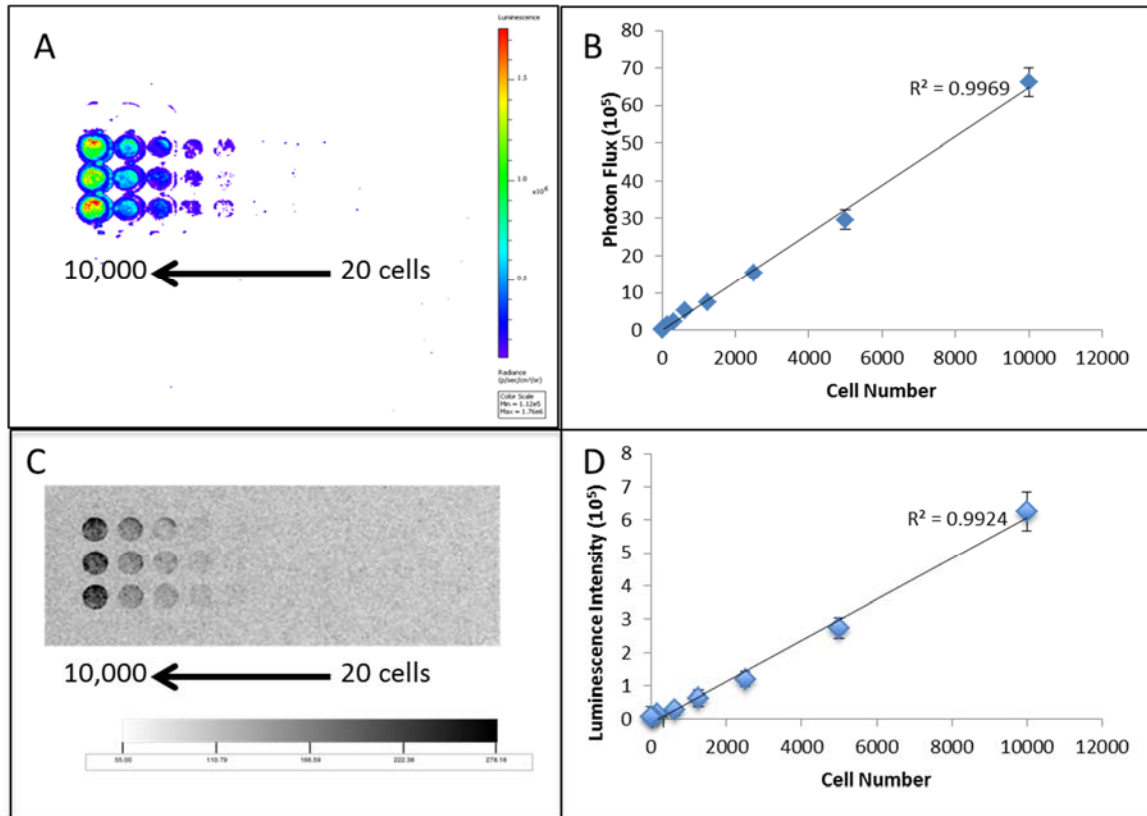


**Figure SI 6. *In vitro* luciferase activity assay in Panc-1 luc cells.** *A.* Heat map of the photon flux (photons per second) detected by IVIS system from serially diluted Panc-1 luc cells, indicating bioluminescent activity. *B.* Luminescence intensity plot as a function of number of Panc-1 luc cells obtained from IVIS imaging. *C.* Bioluminescence activity of Panc-1 luc cells as detected by Kodak FX imaging system. *D.* Luminescence intensity plot as a function of number of Panc-1 luc cells obtained from Kodak FX imaging system. Both plots (*B*, *D*) show a linear correlation between signal intensity obtained as a function of number of cells.

**SI 7. Development of surgical orthotopic pancreatic tumor model:** Nude or SCID beige mice (6 week old, ~20 g body weight) were purchased from Charles River Laboratories (Wilmington, MA) and were allowed to acclimatize for 4-5 days prior to their use. Before surgery, animals were mildly anesthetized by inhalation of 2% IsoSol vapor (St. Joseph, MO) in 100% oxygen. The left side of the SCID mouse was shaved with electric razor till the skin was entirely free of fur and then this area was sterilized with an iodine solution. For implantation of Panc-1 luc cells, a small incision (~1 cm) was made (blade No. 0-15) through the skin and abdominal wall at the base of the spleen. The spleen was gently pulled through the incision, exposing the pancreas. The Panc-1 luc cells in PBS ( $3 \times 10^6$  cells in  $50 \mu\text{L}$ ) were injected into the middle part of pancreas. The cell suspension was allowed to set (~10 sec) and the needle was then withdrawn gently. The surgical area was swabbed with iodine to kill any stray cells at the site of injection. The pancreas and spleen were then replaced in the abdomen and the incision was closed in 2 layers (peritoneum and

abdominal wall) with 4-5 interrupted sutures using absorbable Vicryl sutures (Ethilon 5-0 PS-3, Ethicon, Piscataway, NJ). Mice were allowed to recover on Heat pad. Mice were subcutaneously injected with 0.1 mg/mL Buprenorphine subcutaneously twice per day for 4 days following the surgery and the animals were observed three times/day for checking their movement, physical activity and any sign of discomfort. Live imaging of animals was performed 5 days after surgery to assess tumor formation at the site of injection. Mice were intraperitoneally injected with 200  $\mu$ L of 15 mg/mL D- Luciferin substrate solution, incubated for 10 minutes and were imaged under Lumina II in vivo imaging system (IVIS) from Caliper Life Sciences (Hopkinton, MA).

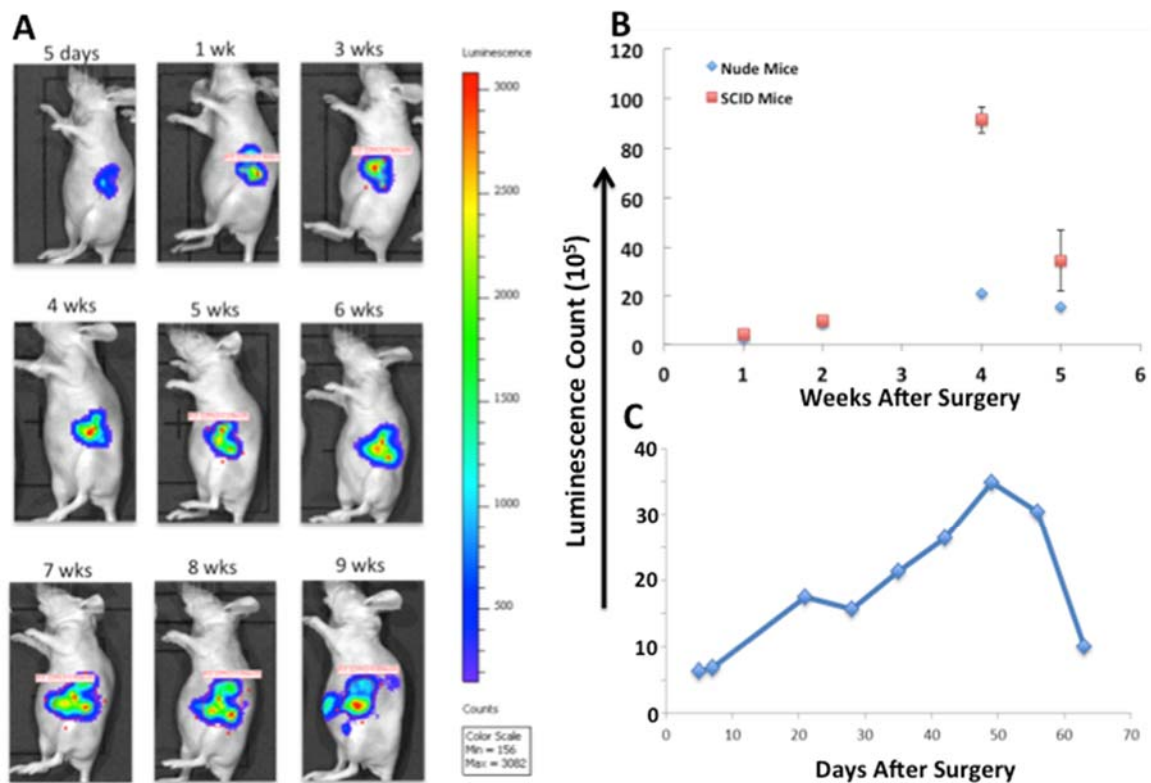


**Figure SI 8. Comparative assessment of orthotopic pancreatic tumor growth and development in nude vs SCID beige mice.** (A) Images of nude mice showing the orthotopic pancreatic tumors measured bioluminescence activity of Panc-1 luc as a function of time by using IVIS imaging. (B) Plot of bioluminescence signal from Panc-1 luc for comparative assessment of tumor growth profile in nude vs SCID beige mice as a function of time. (C) Bioluminescence signal obtained from nude mice alone as a function of time post-surgery. Animals were administered with 200  $\mu$ l of luciferin (15 mg/ml) intraperitoneally, 10 min prior to capturing the images.

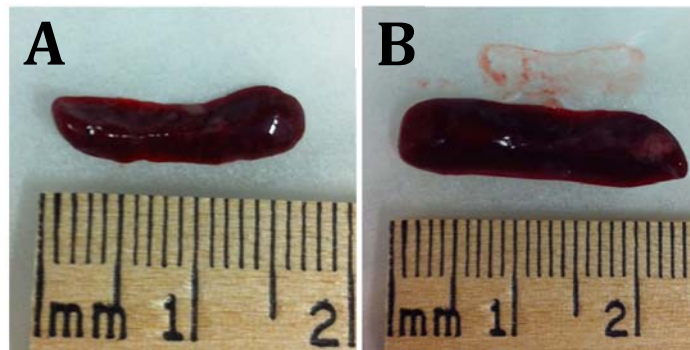


**Figure SI 9.** Splenomegaly was observed in the orthotopic pancreatic tumor bearing mice (B) compared to the spleen from naïve mice (A), suggesting infiltration of cancer cells into the spleen of tumor bearing mice.

Treatment Groups	Number of Animals
PBS Control Group	6
Gem Solution Group	6
Gem in Non-targeted Gelatin Nanoparticles	6
Gem in EGFR-targeted Gelatin Nanoparticles	6

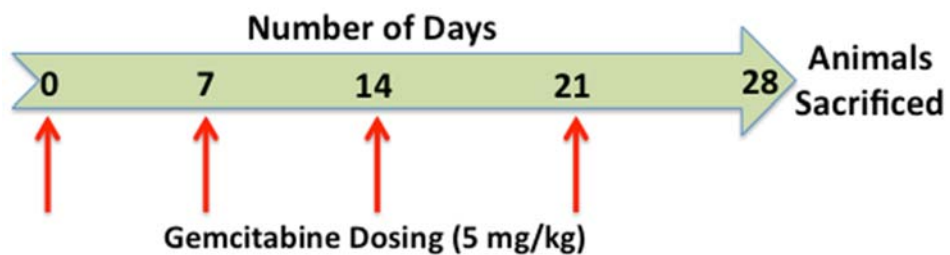


**Figure SI 10. Gemcitabine dosing schedule during efficacy studies.** The orthotopic pancreatic tumor bearing SCID beige mice were intravenously injected with PBS or Gemcitabine formulation (5 mg/kg) at 0, 7, 14 and 21 days and tumor progression was observed by IVIS imaging. The animals were finally sacrificed at day 28.

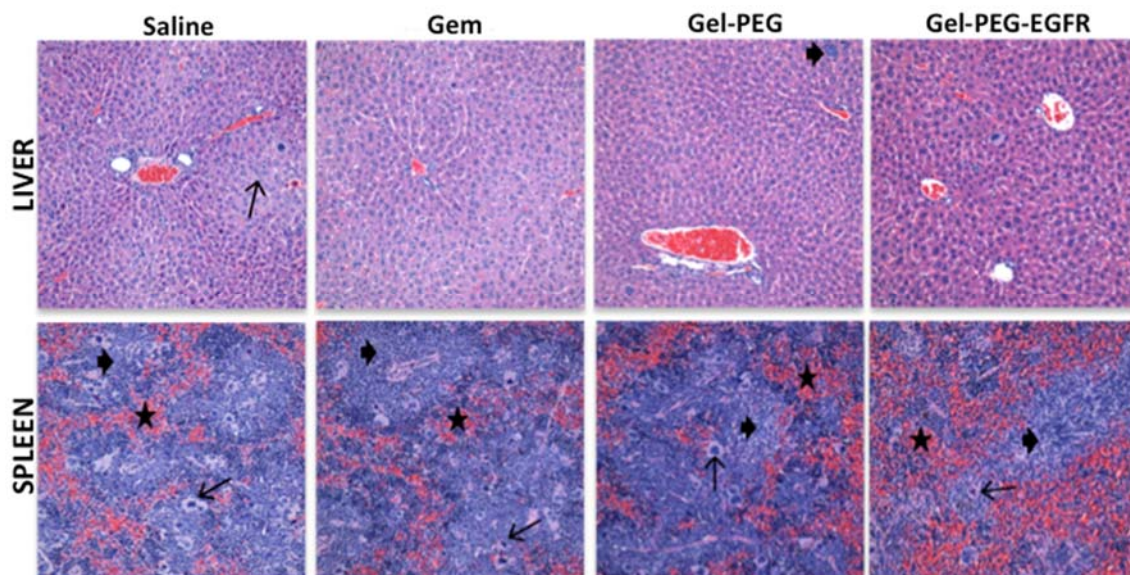


**Figure SI 11. H&E stained imaging of liver (top) and spleen (bottom).** A focal area of extramedullary hematopoiesis is present (arrow) as well as moderate hepatocellular vacuolation (arrowhead) in the section of excised liver. The sections of the excised spleen tissue show red pulp (star) and white pulp (arrowhead) as well as abundant extramedullary hematopoiesis are indicated by many megakaryocytes (arrow). All images were acquired at a magnification of 20X.

The liver tissues from the all treatment groups demonstrate moderate periacinar and diffuse hepatocellular vacuolation (arrows, top panel). Occasional multifocal aggregates of cells (arrowheads, top panel) were present in portal areas consistent with extramedullary hematopoiesis (EMH). The extramedullary hematopoiesis observed is considered as an incidental finding and is not due to potential toxicity of formulations. The spleen tissues from the all treatment groups demonstrated moderate multifocal lymphoid nodular hyperplasia as well as multifocal moderate to marked extramedullary hematopoiesis (arrows, bottom panel). Extramedullary hematopoiesis and lymphoid hyperplasia are common incidental findings in the spleen in mice as are mild EMH and lipid vacuolation in the liver. The tissues examined in treatment groups are consistent with saline control. Histo-pathological characterization indicated that tissues examined in this study are regarded as within normal limits of structural integrity. These results confirm that the gelatin formulations are well tolerated *in vivo*. Although pharmacokinetics study from these nanoparticle formulations revealed high accumulation in livers and spleens, they do not cause any severe damage to these tissues.